

Extracellular Apparent Diffusion in Rat Brain

Timothy Q. Duong,¹ Jonathan V. Sehy,² Dmitriy A. Yablonskiy,^{3,4} B. Joy Snider,⁵ Joseph J.H. Ackerman,^{1,4,6} and Jeffrey J. Neil^{4,7*}

The apparent diffusion coefficients (ADCs) of a series of markers concentrated in the extracellular space of normal rat brain were measured to evaluate, by inference, the ADC of water in the extracellular space. The markers (mannitol, phenylphosphonate, and polyethylene glycols) are defined as “compartment selective” because tissue culture experiments demonstrate some leakage into the intracellular space, making them less “compartment specific” than commonly believed. These primarily extracellular markers have ADCs similar to those of intracellular metabolites of comparable hydrodynamic radius, suggesting that water ADC values in the intra- and extracellular spaces are similar. If this is the case, then it is unlikely that a net shift of water from the extra- to the intracellular space contributes significantly to the reduction in water ADC detected following brain injury. Rather, this reduction is more likely due primarily to a reduction of the ADC of intracellular water associated with injury. Magn Reson Med 45:801–810, 2001. © 2001 Wiley-Liss, Inc.

Key words: diffusion; extracellular space; rat; stroke

Diffusion-weighted imaging (DWI), in which contrast is based on the water apparent diffusion coefficient (ADC), is widely recognized as a useful tool for early detection of brain injury. Its utility in this setting arises from the observation that water ADC decreases rapidly following many forms of acute central nervous system (CNS) injury, including stroke (1), seizure (2), excitotoxic injury (3), trauma (4), hypoglycemia (5), and spreading depression (6). Despite the widespread clinical use of DWI, the pathophysiological mechanism(s) fundamental to changes in the water ADC remains poorly understood.

Water motion in biological tissue is complex. The ADC is a quantification of incoherent molecular displacement which is sensitive to a wide range of incoherent microscopic motions, including passive Brownian thermal dif-

fusion, active transport processes, and macroscopic motions which may include perivascular pulsation, cerebrospinal fluid (CSF) perfusion, and bulk brain motion. Further, water motion may be hindered or restricted by macromolecular binding, barriers such as cell membranes and the cytoskeletal matrix, and high protein concentrations. To complicate matters even more, the CNS water signal, and hence water ADC measurement, arises from molecules exchanging between the intracellular space (ICS) and the extracellular space (ECS), with water in each compartment possibly subject to different motions and barriers to motion. Following brain injury, active transport processes, intra- and extracellular volume fractions, inter-compartment exchange rates, and other factors may change in association with an overall decrease in total water ADC. Due to the complex and unknown factors contributing to water motion in tissue, the descriptor “apparent” is applied to the diffusion coefficient determined by the pulsed-field-gradient method as the MR experimental rate constant characterizing this motion.

The most frequently cited hypothesis explaining the reduction of brain water ADC following injury invokes the net migration of assumed *fast-diffusing* extracellular water into the ICS, an environment of assumed *slow-diffusing* molecules, following cell swelling associated with brain injury (1,7–10). A net migration of a small fraction of total brain water (10%) from the ECS to the ICS with cell swelling could explain the 35–50% ADC decrease commonly observed following cell injury only if apparent diffusion were markedly faster in the ECS than in the ICS, a condition that has not been proven experimentally.

One approach to evaluating mechanisms of water ADC changes is to measure ADCs of metabolically inert endogenous and exogenous molecular species (markers) that can be confined to either the ICS or ECS. Measurements of compartment-specific marker ADCs allow inferential detection of the motional characteristics of water in each compartment. Comparison of water motion in the ICS and ECS can be made if the markers in the two compartments are similar in size (i.e., hydrodynamic radius). Further, marker ADCs can be measured before and after brain injury and their changes taken to reflect similar changes in the motional properties of water in the two compartments.

Recently, we obtained extracellular and intracellular compartment-specific ¹⁹F ADC data from rat brain that suggest the assumption of fast extracellular apparent diffusion and slow intracellular apparent diffusion is incorrect. The ADCs of intracellular and extracellular 2-[¹⁹F]fluoro-2-deoxyglucose-6-phosphate (2FDG-6P) were similar, suggesting that the ADCs of water in both compartments are also similar (11). Further, the motion in both compartments decreased significantly and to a similar degree following global ischemia. These changes imply that a

¹Department of Chemistry, Washington University, St. Louis, Missouri.

²Program in Molecular Cell Biology, Washington University, St. Louis, Missouri.

³Department of Physics, Washington University, St. Louis, Missouri.

⁴Department of Radiology, Washington University School of Medicine, St. Louis, Missouri.

⁵Department of Neurology, Washington University School of Medicine, St. Louis, Missouri.

⁶Department of Internal Medicine, Washington University School of Medicine, St. Louis, Missouri.

⁷Department of Neurology, Division of Pediatric Neurology, St. Louis Children's Hospital, St. Louis, Missouri.

Grant sponsors: McDonnell Center for Higher Brain Function at Washington University; NIH; Grant number: NS35912; Grant sponsor: Dept. of Education Graduate Student Training Grant; Grant number: GAANN, P200A40147-96.

Present address for T.Q. Duong is Center for Magnetic Resonance Research, University of Minnesota School of Medicine, Minneapolis, MN.

*Correspondence to: Jeffrey J. Neil, M.D., Ph.D., Pediatric Neurology, St. Louis Children's Hospital, One Children's Place, St. Louis, MO 63110. E-mail: neil@wuchem.wustl.edu

Received 17 December 1999; revised 19 September 2000; accepted 6 December 2000.

net migration of water from the ECS to the ICS would have little or no effect on the total brain water ADC.

Because the findings of the ^{19}F FDG-6P study are in disagreement with a commonly cited hypothesis, ADC measurements are presented herein of several compartment-selective markers that are ^1H MR-active. To the best of our knowledge, no other *in vivo* MR ADC data representative of the extracellular space have been reported. Low molecular weight (LMW) markers used for extracellular-selective ADC measurements were exogenous mannitol, polyethylene glycol of average molecular weight 200 (PEG-200), and phenylphosphonate (PPA). Mannitol and PPA were chosen because they have often been used as markers of the ECS (12,13). High molecular weight (HMW) extracellular markers were PEG-1000, PEG-2000, and PEG-4600. All markers were directly administered by slow intraventricular infusion. The ADC values for these markers are reported for normal rat brain. Values following global ischemia are not reported for these markers as was done in a preliminary report (14) because they have been found to have relatively poor compartment specificity following injury (as determined in tissue culture preparations by measurement of intracellular concentration following an extracellular challenge, as described below). Nevertheless, the ADC values of these markers from uninjured brain provide unique information for comparison of intra- and extracellular ADC values.

An alternative hypothesis to explain the similar reduction in ADC values for intra- and extracellular markers detected in the ^{19}F FDG-6P study is that the decrease is due to a diminution of brain bulk motion, which should affect both compartments identically (15,16). For example, such a decrease in bulk motion might take place following global ischemia as a result of the loss of arterial pulsation which accompanies cardiac arrest. To evaluate this possibility, changes in the ADC of PEG-4600 (an HMW marker whose ADC should be dominated by bulk motion) were made before and after global ischemia.

Finally, in conjunction with the ADC measurements of the exogenously administered extracellular markers, ADC measurements of an endogenous LMW marker in the intracellular compartment, N-acetyl aspartate (NAA), are reported. These measurements were made both before and after global as well as focal ischemia. They confirm findings published by others (17,18).

MATERIALS AND METHODS

Tissue Culture Preparation and Compartment-Selectivity Assays

Tissue culture experiments were done to evaluate the compartment specificity of the various extracellular marker compounds because data from the literature regarding this specificity are sparse. Mixed neocortical cultures containing similar numbers of neurons and glia were prepared from fetal mice at 14–17 days gestation as previously described (19). Approximately 2.5×10^5 cells per culture well (15 mm diameter) were maintained in the presence of nutrient medium (Eagle's minimal essential medium, 20 mM glucose, 2 mM glutamine, and 10% horse serum) at 37°C in a humidified incubator containing 5% CO_2 and

atmospheric O_2 . Cell cultures were used for experiments 14–16 days after plating.

Each well in a plate of cells was incubated for 4 h in 400 μL of nutrient medium containing 10–50 mM marker (Aldrich, Milwaukee, WI) in a humidified incubator at 5% CO_2 and atmospheric O_2 . Each row of four wells contained a different marker for a total of six markers and 24 wells per plate. The incubation duration was chosen to reflect the time experienced between marker injection and MRS testing in the animal experiments. Marker concentrations bathing cells were chosen based on calculations of concentrations in rat CSF. A second plate was pre-equilibrated on ice and incubated for 5 min in identical medium conditions in room atmosphere. Low temperature will halt most active transport processes and when coupled with a short incubation period allows for a measurement of membrane binding. After marker exposure and incubation, each well of cells was washed four times with 1.25 ml of nutrient medium (absent marker). Cells were lysed with 300 μL of 0.2% sodium dodecyl sulfate (SDS) in D_2O per well. Lysate solutions were collected and stored at 4°C.

NMR Analysis of Tissue Culture Samples

After 1–2 weeks storage, lysate samples were transferred to 5-mm Shigemi NMR tube inserts for quantification of marker concentrations. High-resolution NMR experiments were performed on an 11.75-T Varian Unity system using a simple pulse and collect sequence with water presaturation. Each experiment used $\text{TR} \sim 4T_1$ (measured by inversion recovery in lysate samples) and 128 transients. The D_2O lysate solvent provided the NMR signal for field homogeneity shimming and deuterium field/frequency lock. Receiver frequency tuning and impedance matching, as indicated by the reflected power of the RF coils, were similar for all samples. External reference spectra were collected from at least three concentrations of each marker in D_2O under the same conditions and during the same day as lysate spectra. These reference data were used to generate a signal intensity vs. marker concentration curve from which marker concentration in lysate spectra was calculated.

Animal Preparation

Animals were prepared and markers infused into the extracellular space in a similar fashion for each marker. Sprague Dawley rats (290–330 g) were anesthetized with a loading dose of 35 mg/kg pentobarbital *ip*. Supplemental doses of 6 mg/kg pentobarbital were given at half-hour intervals or as needed. Each animal was placed in a stereotaxic head frame (Kopf, Tujunga, CA) for infusion. Two holes, each 1.5 mm in diameter, were drilled into the skull. Two stainless steel 30-gauge needles were stereotaxically placed in the lateral ventricles at coordinates of ± 1.4 mm lateral to bregma, 0.9 mm posterior from bregma, and 3.5 mm deep from the dura (11). A total of 100–125 μL of 0.15–1.5 M marker in saline was infused into each lateral ventricle simultaneously (i.e., 50–63 μL in each ventricle) over the course of approximately 1 hr.

Following infusion, the femoral vein was catheterized and the trachea was cannulated. A fiber-optic thermal

probe (Luxtron, Santa Clara, CA) was inserted into the nasal cavity of the animal and the temperature maintained at 36–38°C throughout the MR experiment with a circulating water cushion and/or warm air flow. Intranasal temperature measurement agrees with intracerebral temperature measurement to within 1°C (unpublished data). During the MR experiment, the animal was mechanically ventilated with 2–3% (v/v) halothane in 100% O₂ using a rodent respirator (Model 55-2226; Harvard Apparatus, Dover, MA). A toothbar head restraint was employed to reduce motion artifacts.

Three to five repetitive ADC measurements were made with each live rat starting 3–4 hr (for mannitol and PPA) or 4–6 hr (for PEGs) after the conclusion of the intraventricular infusion. The timing was chosen based on previous experience to allow the infusates to distribute throughout the interstitial (extracellular) space. For the global ischemia model, rats were sacrificed by pentobarbital overdose (160 mg/kg, iv) while in the magnet and three to eight additional repetitive ADC measurements were made. Rat brain temperature after death was maintained at 37°C, as described above. Water ADC measurements were interleaved with each marker ADC measurement. A single combined marker and water ADC measurement required 5 min for PEGs and 10 min for mannitol/NAA and PPA.

In a subset of animals, NAA ADC measurements were made after focal ischemic brain injury induced by permanent intraluminal occlusion of the right middle cerebral artery (MCA). This was done to confirm previous studies indicating that the ADC values of intracellular metabolites are reduced following injury. Measurements of ADC started ~5–10 min following the MCA occlusion and continued for ~2 hr. The initial five ADC measurements were made on the hemisphere ipsilateral to the stroke followed by interleaved ADC measurements of contralateral and ipsilateral hemispheres. Water ADC measurements were made between each NAA ADC measurement. A single set of NAA and water ADC measurements required 10 min.

MR Experiments In Vivo

In vivo MR experiments were performed on a 4.7-T, 33-cm diameter clear bore Oxford Instruments magnet equipped with an 18-G/cm, actively-shielded, Oxford Instruments magnetic field gradient set and a Varian ^{UNITY}INOVA console. Sample excitation and signal detection were performed with a 3-cm quadrature rat head coil of birdcage design.

Measurements employed a modified PRESS volume localization sequence with 3× CHES water suppression (3-DRYPRESS) (20). Diffusion sensitizing gradients were placed symmetrically about both π pulses (Fig. 1). Voxel shimming achieved linewidths of 12–18 Hz (0.06–0.09 ppm). Marker ADCs were measured with a typical voxel dimension of 6 × 8 × 5 mm³ for global ischemia and 3 × 4 × 5 mm³ for focal ischemia. Table 1 summarizes the diffusion sequence parameters. In general, the maximum b value for each marker was chosen to approximate one e -fold attenuation of signal amplitude for normal rat brain. The spectra averaged at each b value were collected in an interleaved fashion. Water ADCs from the same voxels were also determined ($b = 4, 504, 974$ s/mm²), with two transients averaged at each b value.

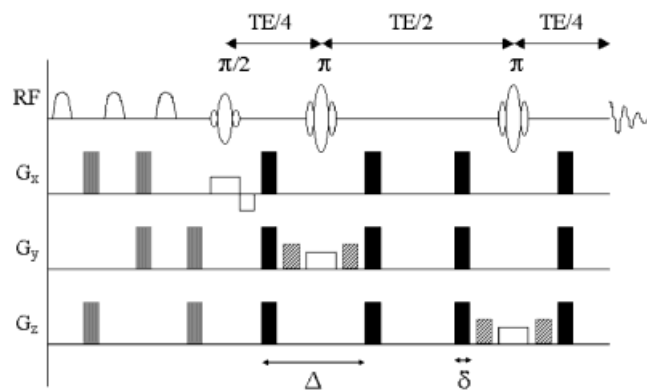


FIG. 1. Schematic representation of a PRESS volume-localized diffusion-spectroscopy pulse sequence employing CHES water suppression. The three CHES elements utilize gaussian-shaped RF pulses followed by crusher gradients (gray rectangles). The excitation and refocusing sinc pulses are applied during slice-selection gradient events (open rectangles). The diffusion-sensitizing magnetic field gradients (black rectangles) are placed symmetrically about each of the two π pulses. Crusher gradients (hatched rectangles) also accompany each of the π pulses. The b values are increased by simultaneously increasing the gradient amplitudes along all three axes. The symbol δ represents the duration of each diffusion-sensitizing gradient pulse and Δ represents the time between application of these gradient pulses. The diffusion time during which the ADC measurement is sensitive to motion is the same for all six main diffusion-sensitizing events. Timings and amplitudes are not drawn to scale.

Free Diffusion Coefficients (D_{free})

The free diffusion coefficients of the compartment markers in aqueous solution (5–20 mM) were measured at 37°C using the Stejskal-Tanner diffusion sequence (21). The values obtained were used for calculation of hydrodynamic radius (R_{HD}) and tortuosity (λ) as described below. Six to eight b values were employed with a delay between acquisitions of $\sim 4T_1$ and 8 or 16 transients averaged at each b value. Other diffusion measurement sequence parameters were similar to those used in vivo, as described above.

Data Analysis

Tissue Culture Data

Marker resonance amplitudes were quantified by frequency-domain resonance integrations of only well-resolved signals. Lysate marker signal amplitudes were fit to standard curves made from external reference integrations to generate lysate marker concentrations. Lysates collected from cells under conditions expected to allow minimal membrane transport allowed for quantification of marker-membrane binding. After dilution factors were considered and membrane binding components were subtracted, intracellular marker concentrations were calculated assuming an intracellular volume of 3.3 pL/cell (11) and 2.5×10^5 cells/well (22).

In Vivo ¹H Diffusion Data

The ¹H spin echo signal amplitude data were modeled by the Stejskal-Tanner equation (21) using nonlinear least-square fitting to the expression:

Table 1
Diffusion Sequence Parameters (TR = 1500)^a

Marker	TE	Δ	δ	t_{diff}	b (s/mm ²)	nt ^b
PPA	60	22	6.0	20.0	1, 1543, 3060	128
PEG-200	70	23	8.1	20.3	11, 3763, 7367	64
PEG-1000	70	23	8.1	20.3	11, 6341, 12477	64
PEG-2000	70	23	7.0	20.7	20, 6259, 11772	64
PEG-4600	70	23	9.0	20.0	12, 8895, 17553	64
Mannitol ^c	60	22	6.0	20.0	1, 1543, 3060	128
Water ^c	60	22	6.0	20.0	4, 504, 974	2
NAA ^c	60	22	6.0	20.0	1, 1543, 3060	128
NAA ^d	60	14	7.0	11.7	4, 1596, 3134	128

^aAll times are given in units of milliseconds.

^bnt is number of transients averaged per b value.

^cADC measurements acquired in the same seven rats. Water ADC measurements were interleaved with those of mannitol and NAA. NAA and water ADC measurements were performed before and after global ischemia.

^dADC measurements were performed before and after focal ischemia.

$$S_i = S_0 \exp(-b_i \cdot \text{ADC}), \quad [1]$$

where S_i is the signal amplitude at the i th b value and S_0 is the echo signal amplitude with $b = 0$. If, as in the original experiments by Stejskal and Tanner, only diffusion-sensitizing gradients are employed, the parameter b_i is given by:

$$b_i = \gamma^2 G_i^2 \delta^2 (\Delta - \delta/3) \quad [2]$$

where γ is the magnetogyric ratio, G_i is the diffusion gradient amplitude, δ is the duration of each gradient pulse, and Δ is the time between application of the two gradient pulses. The quantity $(\Delta - \delta/3)$ is often referred to as the diffusion time (t_{diff}) and defines the time scale during which the ADC measurement is sensitive to motion. In pulse sequences in which other gradients exist (i.e., imaging), cross-term contributions to b values due to interactions between voxel-selection gradients and diffusion gradients should be taken into account (23,24). The exact expression employed was:

$$b_i = \gamma^2 (2aG_s^2 + 6cG_{d,i}^2 + 2dG_c^2 + 2eG_{d,i}G_s + 2fG_{d,i}G_c + 2gG_sG_c) \quad [3a]$$

where

$$a = \delta_s^2 (\Delta_s - \delta_s/3) \quad [3b]$$

$$c = \delta_d^2 (\Delta_d - \delta_d/3) \quad [3c]$$

$$d = \delta_c^2 (\Delta_c - \delta_c/3) \quad [3d]$$

$$e = 2\delta_d \delta_s \Delta_s \quad [3e]$$

$$f = 2\delta_d \delta_c \Delta_c \quad [3f]$$

$$g = 2\delta_c \delta_s \Delta_s, \quad [3g]$$

and the subscripts s , d , and c refer to the slice-selection, diffusion, and crusher gradient events, respectively. The

factor of 6 in front of the second term in Eq. [3a] reflects the six pairs of diffusion-encoding gradients (two pairs on each of three principal axes) as shown in Fig. 1. The factor of 2 in front of the first and third terms reflects the contribution to b values from the slice-selective gradients and crusher, respectively. The fourth, fifth, and sixth terms are the cross-terms among the diffusion, slice-selective, and crusher gradients. Note that only the cross-term interactions between gradients on the same axis were taken into account. In this study, the cross-term contributions arose mainly from the interaction between diffusion gradients and crusher gradients around the π pulses. With the parameters employed here, cross-terms contributed a maximum of $\sim 8\%$ of the b value.

Statistical analyses were performed using repeated (measures of) ANOVA, ANOVA, or Student's t -test.

RESULTS

Extracellular Compartment Selectivity of ¹H MRS-Visible Markers

In vitro tissue culture experiments were performed to measure the extracellular compartment selectivity of markers in a model of normal (i.e., noninfarcted) CNS. Markers bound to cell membranes contributed 44%, 69%, 21%, 39%, 27%, and $<2\%$ to mannitol, PEG-200, PEG-1000, PEG-2000, PEG-4600, and PPA concentrations, respectively, in cell lysates. Table 2 shows the intracellular concentrations of markers present in cells when challenged with extracellular marker-enriched medium. After 4 hr of incubation, markers were selective for the extracellular space (ECS) over the intracellular space (ICS) at concentration ratios of 3–10 to 1. Table 2 includes the calculated content ratios of markers in vivo. This calculation is based on the intra- to extracellular concentration ratios determined in the tissue culture experiments, the degree of nonspecific binding measured in the tissue culture experiments, and the assumption of an 80/20 volume ratio for the intracellular/extracellular volumes in rat brain. These numbers represent an estimate of the proportion of signal arising from each of the three compartments (intracellular, extracellular, membrane-bound) in the in vivo experiments.

Table 2
Extracellular Marker Compartment Specificity

Marker	Tissue culture data		Calculated in vivo distribution*		
	Extracellular concentration (mM)	Intracellular concentration (mM) \pm SD	Nonspecific membrane binding (%)	Extracellular fraction (%)	Intracellular fraction (%)
PPA	50	16.8 \pm 1.2	1	42	57
mannitol	50	11.4 \pm 3.5	27	38	35
PEG-200	50	6.4 \pm 2.8	43	38	19
PEG-1000	20	6.1 \pm 0.2	13	39	48
PEG-2000	10	1.2 \pm 0.3	17	57	26
PEG-4600	10	0.86 \pm 0.10	9	68	23

*Calculation based on a volume ratio of 80/20 between the intra- and extracellular compartments.

Tissue culture experiments were also performed to measure the extracellular compartment selectivity of markers in conditions of oxygen and glucose deprivation (OGD), a model of ischemic injury. With nearly all markers studied, intracellular concentrations rose after ischemic injury (data not shown).

ADC Measurements of Markers In Vivo

To verify the accuracy of ADCs measured using PRESS volume localization, an in vitro control experiment was done in which datasets for measurements of D_{free} were collected using both nonlocalized diffusion measurement pulse sequences and PRESS. The values obtained using the two methods were virtually identical (data not shown). With regard to the in vivo studies, representative ^1H diffusion-weighted spectra of normal rat brain are shown in Fig. 2. Following mannitol infusion, resonances at 3.8 ppm and 2.0 ppm are those of mannitol and NAA, respectively. Following PEG-200 infusion, resonances at 3.8 ppm and

2 ppm are those of PEG-200 and NAA, respectively. Table 3 displays a summary of the diffusion characteristics for these markers. Mean ADCs generated from 12 (mannitol and NAA) or 18 (PEG-4600) b values were virtually identical to measurements using three b values (data not shown) and were well modeled by monoexponential functions in preliminary experiments. In vivo ADCs for LMW markers were $(0.137\text{--}0.22) \times 10^{-3} \text{ mm}^2/\text{s}$. ADCs for HMW markers were $(0.063\text{--}0.091) \times 10^{-3} \text{ mm}^2/\text{s}$. Table 3 includes calculated values for R_{HD} and λ . Values for λ were corrected for nonspecific tissue binding. This was done using the expressions:

$$ADC_{\text{in vivo}} = f_{mb}ADC_{mb} + (1 - f_{mb})ADC_{\text{corrected}} \quad [4]$$

and

$$\lambda_{\text{corrected}} = \sqrt{D_{\text{free}}/ADC_{\text{corrected}}} \quad [5]$$

where f_{mb} and ADC_{mb} represent the fraction of marker nonspecifically bound to membrane (Table 2) and the ADC value for cell membrane components [taken as $0.02 \times 10^{-3} \text{ mm}^2/\text{s}$ (25)], respectively. $ADC_{\text{in vivo}}$ is the ADC value for the marker measured in brain.

The change in ADC during global or focal ischemia for NAA is shown in Table 4, together with ADC changes during global ischemia of two other ICS markers, 2FDG-6P and Cs^+ . NAA and 2FDG-6P have ADCs in normal CNS that are similar to those of the ECS markers of comparable R_{HD} described in Table 3. The ADCs of the ICS markers fall following death ($P < 0.01$, ANOVA) and remain unchanged for up to 0.5–1 hr. After global ischemia, the ADC of NAA decreases 25%. After focal ischemia, the ADC of NAA decreases to a lesser extent (17%). The drop after focal ischemia develops quickly ($\sim 5\text{--}10$ min) with no further significant decrease observed as late as 2 hr after injury. Note that the ADC of the largest marker, PEG-4600, dropped from $(0.063 \pm 0.002) \times 10^{-3} \text{ mm}^2/\text{s}$ to $(0.042 \pm 0.003) \times 10^{-3} \text{ mm}^2/\text{s}$ after global ischemia.

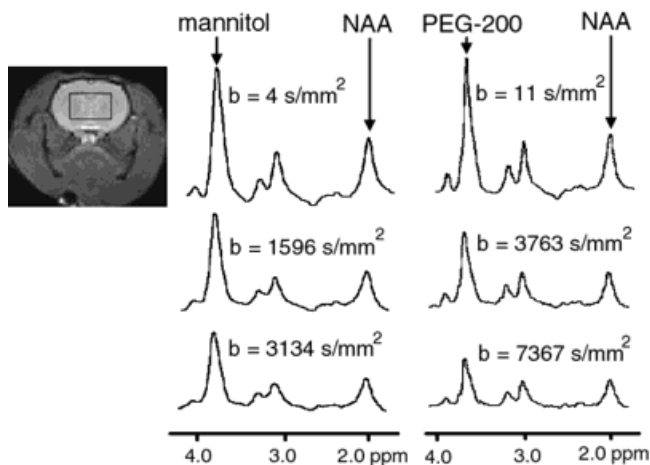


FIG. 2. ^1H MR of compartment-selective markers. Left: A coronal image of a rat brain showing a typical region of interest (ROI) used in obtaining diffusion-weighted spectra in normal and globally ischemic CNS. Right: A series of representative diffusion-weighted, volume-localized ^1H spectra from normal rat brain. A 1–2 Hz line broadening time domain exponential apodizing filter has been applied. The spin-echo amplitudes attenuate with increasing b values as expected. Assignments: mannitol at 3.8 ppm, PEG-200 at 3.8, choline at 3.2 ppm, Cr/PCr at 3.0 ppm, and NAA at 2.0 ppm.

DISCUSSION

Marker Characteristics

In this study, changes in the ADC values of markers were used to infer the motional characteristics of the extra- and

Table 3
In Vivo Diffusion Parameters for Markers

Marker	MW	$D_{\text{free}}^{\text{a}}$ (10^{-3} mm ² /s)	R_{HD}^{b} (Å)	ADC _{in vivo} (10^{-3} mm ² /s) mean ± SD (n)	Tortuosity ^c (λ)	Corrected tortuosity ^d (λ _{corrected})
PPA	158	0.68	4.8	0.22 ± 0.01 (4)	1.76	1.75
Mannitol	182	0.90	3.6	0.20 ± 0.01 (4)	2.12	1.83
PEG-200	200	0.74	4.4	0.137 ± 0.004 (4)	2.32	1.81
PEG-1000	1000	0.33	10.0	0.091 ± 0.002 (7)	1.90	1.80
PEG-2000	2000	0.14	23.5	0.077 ± 0.002 (5)	1.35	1.26
PEG-4600	4600	0.12	27.4	0.063 ± 0.002 (5)	1.38	1.34

^a D_{free} was calculated in dilute aqueous solution at 37°C.

^bHydrodynamic radius (R_{HD}) was calculated from D_{free} using the Stokes-Einstein equation $R_{\text{HD}} = kT/6\pi\eta D_{\text{free}}$.

^cTortuosity (λ) is defined as $\sqrt{D_{\text{free}}/\text{ADC}}$.

^dTortuosity corrected for the bound fraction of marker. See text for details.

intracellular spaces. An ideal “compartment-specific” marker would be completely confined to the compartment of interest (in this case, the extracellular space). Markers were chosen for this study because they have been used in other studies as compartment-specific indicators, but the tissue culture experiments reported here indicate that many commonly used markers of the extracellular compartment experience more leakage into the intracellular space than is commonly believed. Nonetheless, signal arising from the extracellular space comprised 40–70% of total signal for the markers employed in this study (assuming that the ECS comprises approximately 20% of the rat CNS volume). This is a percentage substantially higher than the 20% typical of water. Therefore, we describe our inert markers as “compartment-selective,” a grouping we consider distinct from that of a marker such as 2FDG-6P, which we have shown to be compartment-specific. For comparison, tissue culture experiments indicated that 90% of the total in vivo rat marker signal arose from 2FDG-6P in the ECS (11).

The assumption that mixed cortical tissue culture obtained from fetal mice is a reasonable model for adult rodent brain is implicit in this discussion. This particular system was chosen because it is well-characterized. Membrane permeability characteristics are likely to be similar between the tissue culture system employed and rat brain (19).

An ideal marker would also have no nonspecific membrane binding. The markers used in this study had membrane binding ranging from 1–43% of total signal. As a result of this binding, an attempt was made to correct the

calculated tortuosities. Whether this nonspecific binding is due to interaction of the marker with charged molecules on the membrane surface or incorporation of the marker into the lipid bilayer itself cannot be determined from this study. Again for comparison, 2FDG-6P had membrane binding of 12% (11).

Finally, an ideal marker would be present in low enough concentration that it is not osmotically active. The compounds used for this study likely had some degree of osmotic activity, which would serve to draw water into the extracellular space. The addition of water to the extracellular space would be expected to reduce the measured tortuosity there. However, markers infused at lower concentrations (PEG-2000, PEG-4600) gave lower tortuosities rather than higher, indicating that this effect is likely small.

With regard to the measurement method used, the extracellular ADCs measured here may include contributions from marker contained in the relatively unrestricted cerebroventricular space. The PRESS voxel for normal CNS included the lateral ventricles, but all ventricular volumes together likely constitute only about 7% of extracellular water volume in rat brain (26). ADCs measured from smaller voxels avoiding the lateral ventricles confirm that any ADC contribution from the cerebroventricular space is minor. The signal from the smaller voxels suffered a lower SNR per unit acquisition time, but ADCs were unchanged from those of the larger voxels used here (data not shown). The subarachnoid spaces surrounding the brain were not included in the CNS PRESS voxel.

Table 4
Water and Intracellular Marker Apparent Diffusion in Normal and Ischemic CNS

Marker	MW	D_{free} (10^{-3} mm ² /s)	R_{HD} (Å)	ADC (10^{-3} mm ² /s)		% Decrease	λ	
				Normal (n)	Ischemic		Live	Dead
NAA	175	0.93	3.5	0.16 ± 0.01 (7) ^a	0.12 ± 0.02	25	2.4	2.8
				0.18 ± 0.03 (5) ^b	0.15 ± 0.03	17	2.3	2.5
2FDG-6P ^c	260	0.70	4.7	0.16 ± 0.03 (7) ^a	0.10 ± 0.02	38	2.1	2.6
Cs ⁺ ^d	133	2.7	1.2	0.91 ± 0.05 (5) ^a	0.64 ± 0.02	30	1.7	2.1
Water	18	3.0	1.1	0.80 ± 0.02 (7) ^a	0.50 ± 0.02	38	1.9	2.4

^aGlobal ischemia.

^bFocal ischemia. “Normal” refers to the contralateral hemisphere during ipsilateral MCA occlusion.

^cData from Ref. 11.

^dData from Ref. 36. Measured D_{free} was 1.9×10^{-3} mm²/s (22°C). The D_{free} value reported here was corrected for temperature.

Extracellular Tortuosity

The values for tortuosity in the extracellular space determined using the smaller markers (mannitol, PPA, PEG-200, PEG-1000) range from 1.75–1.83. This is somewhat higher than most literature values, which are on the order of 1.5–1.6 (27). When comparing the values for λ obtained in this study to others, it is instructive to compare the methodologies used.

One difference between the MR method used here and those used in other studies lies in the distance scale over which the measurement is made. The root-mean-squared (RMS) displacement of a molecule in one dimension as typically measured using the pulse-field-gradient method (for example, along the x-axis), is given by:

$$\langle x^2 \rangle^{1/2} = \sqrt{2\text{ADC}(\Delta - \delta/3)} = \sqrt{2\text{ADC}t_{\text{diff}}} \quad [6]$$

where t_{diff} is the diffusion time. Assuming isotropic motion, the RMS displacement in three dimensions is given by:

$$\langle r^2 \rangle^{1/2} = \sqrt{6\text{ADC}t_{\text{diff}}}. \quad [7]$$

The diffusion time for the MR experiments described here is 20 ms, giving an RMS displacement for the LMW markers on the order of 4–5 μm . Other methods for measuring diffusion entail greater mean square displacements. Typical radiotracer studies involve distances on the order of mm. Tetramethylammonium and integrative optical imaging studies involve distances on the order of hundreds of μm . Yet the 4- μm displacement of the MR measurement is still considerably greater than the average spacing between cell membranes in the interstitial space, which is on the order of 10–30 nm (28). Thus, the markers (or water) have frequent encounters with cell membranes which would hinder their diffusion, even during the MR experiment.

The difference in distance scale should have an effect on the values for λ only if there are barriers to cell motion that are inhomogeneous over distances of at least tens of μm . Whether or not such inhomogeneity exists is not clear. It has been suggested that markers may move relatively great distances within the perivascular spaces and perivascular pulsation-driven transport in the brain extracellular space has been demonstrated in many laboratories (29–31). Arteries and veins are enclosed in a fluid-filled perivascular space continuous with the subarachnoid space. Capillaries lack such a surrounding space. Rennels et al. (30) observed that the distribution of horseradish peroxidase (HRP) after intraventricular infusion is too rapid to be explained by simple diffusion. Within 6 min of injection of the 44-kDa enzyme into the subarachnoid space, the periarteriole space was labeled. Within a few hours, both the periarteriole and the perivenule spaces were labeled. Time-lapse profiles of the HRP distribution suggest that HRP movement is directional (from subarachnoid space to periarteriole space to capillary basal lamina to perivenule space). The authors propose that this movement is powered by perivascular pulsation. Assuming that this is the case, it is possible that relatively few of the marker molecules would sample this space during the MR experiment because of the smaller RMS displacements during such studies rela-

tive to the distance between noncapillary vessels with perivascular spaces. This would tend to give higher values for λ in the MR experiment.

Another potential explanation for the slightly higher values for λ in this study lies in the compartment specificity. Our “extracellular” markers are not confined completely to the extracellular space, but are contained in the intracellular space as well. While some authors believe that λ values are similar for the two spaces (32), it is conceivable that λ for the intracellular space is somewhat higher than for extracellular. If this is the case, λ for markers which enter the intracellular space would be somewhat higher than λ for markers which are confined to the extracellular space. Arguing against this, the degree of intracellular leakage does not correlate with λ in this study. PPA and PEG-200 have the highest and lowest extracellular fractions, respectively (Table 2), yet they have virtually identical values for $\lambda_{\text{corrected}}$ (Table 3). Thus, this effect is likely to be a minor one.

To the best of our knowledge, no other in vivo ADCs representative of the extracellular space employing MR have been reported by other laboratories. Thus, cross-laboratory comparison is not available. However, the values for λ reported here are somewhat lower than those previously reported by our laboratory for extracellular 2FDG-6P determined by ^{19}F MRS (11), which gave an $\text{ADC}_{\text{in vivo}}$ of $0.144 \times 10^{-3} \text{ mm}^2/\text{s}$, λ of 2.2, and $\lambda_{\text{corrected}}$ of 2.1 (with 12% nonspecific membrane binding). The present study was, in large part, motivated by a desire to explore the extracellular space with markers differing chemically from 2FDG-6-P and the reason for the discrepancy in λ values may lie in the chemical properties of the markers. 2FDG-6-P contains a negatively charged phosphate group which could interact with positive charges on cell membranes. This is relatively improbable because the charges on cell membranes are likely to be negative (33).

The two larger MW markers, PEG-2000 and PEG-4600, give λ values of approximately 1.3. These values are lower than those for the lower molecular weight markers reported in this study (1.75–1.83) and given in the literature [1.5–1.6 (27)]. It is unlikely that the difference is related to compartment specificity, as the intracellular/extracellular ratios for these markers are similar to those of the other markers. There are several other possible explanations for this finding. One relates to possible perfusion of markers through the extracellular space (as opposed to the perivascular space). If extracellular fluid perfusion exists and is relatively slow, displacement due to perfusion would become more noticeable or dominant for markers which have low values for D_{free} and are small enough to fit easily through the ECS. Such markers would give lower values for $D_{\text{free}}/\text{ADC}$, or λ . Another possible explanation lies in the conformation assumed by PEG molecules or their effect on water viscosity. The higher molecular weight forms tend to assume a random coil form which may fit through the tortuous extracellular space more efficiently (34). Further, the addition of relatively low concentrations of higher molecular weight PEG to water reduces the frictional resistance to water flow (35). Which, if any, of these explanations is true cannot be determined from the present study.

Intracellular Motion

Our data on the diffusion of NAA give an intracellular tortuosity of approximately 2.3. This value is in reasonable agreement with that for intracellular 2FDG-6-P of 2.1 (11) but is somewhat higher than that for intracellular $^{133}\text{Cs}^+$, which is 1.7 (36). This discrepancy may again lie in the chemical properties of the marker molecules. $^{133}\text{Cs}^+$ has a somewhat loosely associated hydration shell in aqueous solution as well as a relatively high D_{free} because it does not hydrogen bond as strongly as other cations such as Na^+ . It is conceivable that the intracellular λ for $^{133}\text{Cs}^+$ represents a lower limit for water in the intracellular space if $^{133}\text{Cs}^+$ tends to stay in solution rather than bind to more slowly-moving intracellular constituents.

ADC Change Following Brain Injury

It is widely accepted that brain water ADC values fall following a variety of forms of brain injury. The mechanism underlying this change, however, remains the subject of active debate. The most commonly cited hypothesis is that the change in ADC is due to a net shift of water from the “fast-diffusing” extracellular space to the “slow-diffusing” intracellular space as a consequence of cell swelling. If the ADC is viewed as a weighted average of the ADCs of water in the intracellular and extracellular spaces, the average is weighted more to intracellular diffusion and, as a result, the measured ADC decreases. One of the assumptions underlying this volume-shift hypothesis is that diffusion is significantly “slower” in the intracellular space than extracellular. Put another way, the intracellular tortuosity is significantly higher than extracellular. For this mechanism to explain the ~30% decrease in ADC associated with brain injury, ADC values for water in the extracellular space would need to be close to those of free water. This is clearly not the case, as values for λ in the extracellular space are significantly greater than unity. Further, values for λ in the two spaces may be quite similar (32). Thus, we feel this hypothesis is probably incorrect.

Another mechanism which may contribute to the ADC decrease associated with brain injury is a reduction of bulk brain displacement. Such a macroscopic motion may be associated with respiratory movement and/or brain pulsation (perhaps driven by cardiac pulsation) and would be expected to contribute a similar absolute amount to the ADC of any molecule, independent of size. For a given compartment, such as the ECS, one may express the apparent diffusion coefficient as the sum of the rate constants reflecting each independent displacement mechanism:

$$\text{ADC}_{\text{ECS}}^{\text{total}} = \text{ADC}_{\text{ECS}}^{\text{bulk motion}} + \text{ADC}_{\text{ECS}}^{\text{Brownian}} + \text{ADC}_{\text{ECS}}^{\text{perivascular perfusion}} + \text{ADC}_{\text{ECS}}^{\text{CSF perfusion}} + \dots \quad [8]$$

where each ADC describes the displacement mechanism in its superscript. The large hydrodynamic radius of PEG-4600 minimizes $\text{ADC}_{\text{ECS}}^{\text{Brownian}}$ and other size-dependent displacement mechanisms. Thus, of all the markers employed herein its total ADC is most likely to be dominated by bulk brain motion. The decrease of the PEG-4600 ADC following global ischemia is $(0.021 \pm 0.004) \times 10^{-3} \text{ mm}^2/\text{s}$. This decrease suggests that the loss of bulk brain

motion in rat contributes no more than 7% to the water ADC decrease of $0.30 \times 10^{-3} \text{ mm}^2/\text{s}$ following injury.

An alternative hypothesis is that there is a decrease in intracellular motion (intracellular water ADC) associated with cell injury and this leads to the observed overall decrease in water ADC. This is supported by studies on intracellular NAA (17,18), $^{133}\text{Cs}^+$ (36), and 2FDG-6-P (11), which indicate that their ADC values—and, by inference, that of intracellular water—decrease following injury. Our NAA data confirm these findings.

It should be noted, however, that the ADC of 2FDG-6-P in the extracellular space also decreases in association with those forms of injury involving cell swelling (11), suggesting that the ADC of water in this compartment decreases as well. Thus, the available evidence indicates that the water ADC decreases in *both* spaces following injury, although the fraction of water in the extracellular space is less than one-fourth that of intracellular water. Based on the relative volume fractions of water in the two spaces, the decrease in intracellular water ADC would be expected to dominate the observed overall decrease in water ADC. If this is correct, a decrease in intracellular motion, possibly associated with metabolic stress or energy failure, might explain the ADC decrease. The precise mechanism by which intracellular motion changes is unknown. Possibilities include reduced cytoplasmic streaming or changes in effective “viscosity.” One means by which “viscosity” might change is due to breakdown of large macromolecules into smaller species, although whether this would cause an increase or decrease in water ADC depends on the nature of the interaction between the water molecules and macromolecules and their breakdown products. It is also possible that local pH changes lead to protein conformation changes which, in turn, decrease viscosity.

One final possible mechanism relates to changes in extracellular volume. In the effective medium theory, Latour et al. (37) propose that the overall water ADC can be dominated by extracellular motion under certain circumstances. In this case, cell swelling without changes in free diffusion values (i.e., diffusion values in each compartment in the absence of cell membranes) for either the intracellular or extracellular compartment would be sufficient to cause a decrease in overall water ADC. This model has yet to be proven or disproven in intact brain.

Implications for Biexponential Fitting of Water ADC Data

Efforts have been made to use biexponential fitting of water diffusion spin echo amplitude signal attenuation curves to determine water compartmental ADCs in vitro and in vivo. Niendorf et al. (38), in a study of normal rat brain, obtained ADCs (and content fractions) of $0.88 \times 10^{-3} \text{ mm}^2/\text{s}$ (83%) and $0.17 \times 10^{-3} \text{ mm}^2/\text{s}$ (17%). The estimated water content fractions in normal rat brain, as noted by the authors, are the reverse of the expected 80:20 intracellular-to-extracellular volume ratio (if the smaller ADC is assumed to be that of intracellular water). However, the ADC of $0.88 \times 10^{-3} \text{ mm}^2/\text{s}$ is similar to that of intracellular $^{133}\text{Cs}^+$ (36). Thus, it is possible that their value of $0.88 \times 10^{-3} \text{ mm}^2/\text{s}$ represents intracellular water. This interpretation would lead to the expected compart-

ment volume fractions. Our data of compartment markers suggest that intra- and extracellular water ADCs are similar. Thus, it would be challenging to resolve them directly by biexponential fitting. Additionally, this approach is only valid for compartments that exhibit minimal exchange during the diffusion time unless a full compartmental exchange model is employed (39).

CONCLUSIONS

The markers employed are less compartment-specific than generally believed and, hence, we refer to them as “compartment-selective.” The λ values for the extracellular space measured in this study bracket those measured by other methods, with some markers giving values for λ that are higher and some giving values that are lower than alternative methods. The reason for this variability may lie in differences in the chemical structure/conformation of the individual markers and/or the mechanism(s) by which molecules move through the perivascular extracellular space. Overall, λ values for the extracellular space are substantially greater than unity, implying significant restriction to water motion in the extracellular space. As a result, we propose that the primary mechanism by which overall ADC decreases in association with brain injury is a decrease in the intracellular water ADC.

ACKNOWLEDGMENTS

The authors thank Yong Y. He for instruction regarding the intraluminal occlusion focal ischemia model, André d’Avignon for aid in obtaining high-resolution NMR data of cell extracts, Dennis Choi for access to the tissue culture facility and materials, and Ben Woods for technical assistance. Supported in part by a Graduate Student Training Grant (GAANN, P200A40147-96) from the Department of Education to T.Q.D.

REFERENCES

- Moseley ME, Cohen Y, Mintonovitch J, Chileuitt L, Shimizu H, Kucharczyk J, Wendland MF, Weinstein PR. Early detection of regional cerebral ischemia in cats: comparison of diffusion- and T₂-weighted MRI and spectroscopy. *Magn Reson Med* 1990;14:330–346.
- Zhong J, Petroff OAC, Prichard JW, Gore JC. Barbiturate-reversible reduction of water diffusion coefficient in flurothyl-induced status epilepticus in rats. *Magn Reson Med* 1995;33:253–256.
- Verheul HB, Balazs R, van der Sprenkel JWB, Tulleken CAF, Nicolay K, van Lookeren Campagne M. Temporal evolution of NMDA-induced excitotoxicity in the neonatal rat brain measured with ¹H nuclear magnetic resonance imaging. *Brain Res* 1993;618:203–212.
- Ford JC, Hackney DB, Alsop DC, Jara H, Joseph PM, Hand CM, Black P. MRI characterization of diffusion coefficients in a rat spinal cord injury model. *Magn Reson Med* 1994;31:488–494.
- Hasegawa Y, Formato JE, Latour LL, Gutierrez JA, Liu KF, Garcia JH, Sotak CH, Fisher M. Severe transient hypoglycemia causes reversible change in the apparent diffusion coefficient of water. *Stroke* 1996;27:1648–1655.
- Takano K, Latour LL, Formato JE, Carano RAD, Helmer KG, Hasegawa Y, Sotak CH, Fisher M. The role of spreading depression in focal ischemia evaluated by diffusion mapping. *Ann Neurol* 1996;39:308–318.
- O’Shea JM, Williams SR, van Bruggen N, Gardner-Medwin AR. Apparent diffusion coefficient and MR relaxation during osmotic manipulation in isolated turtle cerebellum. *Magn Reson Med* 2000;44:427–432.
- Anderson AW, Zhong J, Petroff OAC, Szafer A, Ransom BR, Prichard JW, Gore JC. Effects of osmotically driven cell volume changes on diffusion-weighted imaging in rat optic nerve. *Magn Reson Med* 1996;35:162–167.
- van Gelderen P, de Vleeschouwer MHM, DesPres D, Parker J, van Zijl PCM, Moonen CTW. Water diffusion and acute stroke. *Magn Reson Med* 1994;31:154–163.
- Benveniste H, Hedlund LW, Johnson GA. Mechanism of detection of acute cerebral ischemia in rats by diffusion-weighted magnetic resonance spectroscopy. *Stroke* 1992;23:746–754.
- Duong TQ, Ackerman JJH, Ying HS, Neil JJ. Evaluation of extra- and intracellular apparent diffusion in normal and globally ischemic rat brain via ¹⁹F NMR. *Magn Reson Med* 1998;40:1–13.
- Colet JM, Makos JD, Malloy CR, Sherry AD. Determination of the intracellular sodium concentration in perfused mouse liver by ³¹P and ²³Na magnetic resonance spectroscopy. *Magn Reson Med* 1998;39:155–159.
- Dobson GP, Cieslar JH. Intracellular, interstitial and plasma spaces in the rat myocardium in vivo. *J Mol Cell Cardiol* 1997;29:3357–3363.
- Duong TQ, Ackerman JJH, Yablonskiy D, Neil JJ. Evaluation of compartment-specific motion in normal and globally-ischemic rat brain via ¹H MRS. In: Proc 6th Scientific Meeting ISMRM, Sydney, Australia, 1998. p 1253.
- Poncelet BP, Wedeen VJ, Weisskoff RM, Cohen MS. Brain parenchyma motion: measurement with cine echo-planar MR imaging. *Radiology* 1992;185:645–651.
- Wirestam R, Greitz D, Thomsen C, Brockstedt S, Olsson MB, Stahlberg F. Theoretical and experimental evaluation of phase-dispersion effects caused by brain motion in diffusion and perfusion MR imaging. *J Magn Reson Imag* 1996;6:348–355.
- Wick M, Nagatomo Y, Prielmeier F, Frahm J. Alteration of intracellular metabolite diffusion in rat brain in vivo during ischemia and reperfusion. *Stroke* 1995;26:1930–1933.
- van der Toorn A, Dijkhuizen RM, Tulleken CA, Nicolay K. Diffusion of metabolites in normal and ischemic rat brain measured by localized ¹H MRS. *Magn Reson Med* 1996;36:914–922.
- Rose K, Choi DW, Goldberg MP. Cytotoxicity in murine neocortical cell culture. In: Tyson J, editor. *In vitro biological methods*. San Diego: Academic Press; 1993. p 46–60.
- Moonen C, van Zijl P. Highly effective water suppression for in vivo proton NMR spectroscopy (DRYSTEAM). *J Magn Reson* 1990;88:28–41.
- Stejskal EO, Tanner JE. Spin diffusion measurements: spin echoes in the presence of time-dependent field gradients. *J Chem Phys* 1965;42:288–292.
- Dugan LL, Bruno VM, Amagasa SM, Giffard RG. Glia modulate the response of murine cortical neurons to excitotoxicity: glia exacerbate AMPA neurotoxicity. *J Neurosci* 1995;15:4545–4555.
- Neeman M, Freyer JP, Sillerud LO. Pulsed-gradient spin-echo diffusion studies in NMR imaging. Effects of the imaging gradients on the determination of diffusion coefficients. *J Magn Reson* 1990;90:303–312.
- Basser PJ, Mattiello J, Le Bihan D. Estimation of the effective self-diffusion tensor from the NMR spin echo. *J Magn Reson B* 1994;103:247–254.
- Reed RA, Mattai J, Shipley GG. Interaction of cholera toxin and ganglioside GM1 receptors in supported lipid monolayers. *Biochemistry* 1987;26:824–832.
- Johanson CE. Ventricles and cerebrospinal fluid. In: Conn PM, editor. *Neuroscience in medicine*. Philadelphia: Lippincott; 1995. p 171–196.
- Nicholson C, Sykova E. Extracellular space structure revealed by diffusion analysis. *Trends Neurosci* 1998;21:207–215.
- Rosenberg GA. *Anatomy of brain interfaces, brain fluids and metabolism*. New York: Oxford University Press; 1990. p 15–35.
- Cserr HF, Cooper DN, Milhorat TH. Flow of cerebral interstitial fluid as indicated by the removal of extracellular markers from rat caudate nucleus. *Exp Eye Res* 1977;25:461–473.
- Rennels ML, Gregory TF, Blaumanis OR, Fujimoto K, Grady PA. Evidence for a ‘paravascular’ fluid circulation in the mammalian central nervous system, provided by the rapid distribution of tracer protein throughout the brain from the subarachnoid space. *Brain Res* 1985;326:47–63.

31. Rennels ML, Blaumanis OR, Grady PA. Rapid solute transport throughout the brain via paravascular fluid pathways. *Adv Neurol* 1990;52:431–439.
32. Nicholson C, Tao L. Hindered diffusion of high molecular weight compounds in brain extracellular microenvironment measured with integrative optical imaging. *Biophys J* 1993;65:2277–2290.
33. Margolis RU, Aquino DA, Klinger MM, Ripellino JA, Margolis RK. Structure and localization of nervous tissue proteoglycans. *Ann NY Acad Sci* 1986;481:46–54.
34. Bahri H, Guveli DE. Viscosity B coefficients of polyethylene glycols in water. *Coll Polym Sci* 1988;266:141–144.
35. Bailey FE, Koleske JV. *Poly(ethylene oxide)*. New York: Academic Press; 1976. p 74–81.
36. Neil JJ, Duong TQ, Ackerman JHH. Evaluation of intracellular diffusion in rat brain via ^{133}Cs NMR. *Magn Reson Med* 1996;35:329–335.
37. Latour LL, Svoboda K, Mitra PP, Sotak CH. Time-dependent diffusion of water in biological model system. *Proc Natl Acad Sci USA* 1994;91:1229–1233.
38. Niendorf T, Dijkhuizen RM, Norris DG, van Lookeren Campagne M, Nicolay K. Biexponential diffusion attenuation in various states of brain tissue: implications for diffusion-weighted imaging. *Magn Reson Med* 1996;36:847–857.
39. Karger J, Pfeifer H, Heink W. Principles and application of self-diffusion measurements by nuclear magnetic resonance. *Adv Magn Reson* 1988;12:1–89.